The Astrophysical Journal, 657: L81–L84, 2007 March 10

X-RAY/UV/OPTICAL FOLLOW-UP OF THE BLAZAR PKS 2155−304 AFTER THE GIANT TeV FLARES OF 2006 JULY

L. Foschini,[1] G. Ghisellini,[2] F. Tavecchio,[2] A. Treves,[3] L. Maraschi,[2] M. Gliozzi,[4] C. M. Raiteri,[5] M. Villata,[5] E. Pian,[6] G. Tagliaferri,[2] G. Tosti,[7] R. M. Sambruna,[8] G. Malaguti,[1] G. Di Cocco,[1] and P. Giommi[9]

Received 2006 December 22; accepted 2007 January 30; published 2007 February 21

ABSTRACT

We present all the publicly available data, from optical/UV wavelengths (UVOT) to X-rays (XRT, BAT), obtained from *Swift* observations of the blazar PKS 2155−304, performed in response to the rapid alert sent out after the strong TeV activity (up to 17 crab flux level at $E > 200$ GeV) at the end of 2006 July. The X-ray flux increased by a factor of 5 in the 0.3–10 keV energy band and by a factor of 1.5 at optical/UV wavelengths, with roughly 1 day of delay. The comparison of the spectral energy distribution built with data quasi-simultaneous to the TeV detections shows an increase of the overall normalization with respect to archival data but only a small shift of the frequency of the synchrotron peak that remains consistent with the values reported in past observations when the TeV activity was much weaker.

Subject headings: BL Lacertae objects: general — BL Lacertae objects: individual (PKS 2155−304)

Online material: color figure

1. INTRODUCTION

PKS 2155−304 ($z = 0.116$) is one of the best known blazars and the second brightest in X-rays (after Mrk 421), observed many times at various wavelengths. At γ-ray energies, it was first detected by the *Compton Gamma Ray Observatory* EGRET with a photon index $\Gamma = 1.71 \pm 0.24$ in the energy range 0.03–10 GeV (Vestrand et al. 1995). This hard spectrum suggested a possible detection in the TeV energy range (Vestrand et al. 1995; Stecker et al. 1996; Tavecchio et al. 1998) that was first achieved by the University of Durham Mark 6 Cerenkov telescope in 1996–1997 (Chadwick et al. 1999).

In 2002–2003, the TeV activity was monitored by the High Energy Stereoscopic System (HESS),[10] which detected a flux variation in the $E > 300$ GeV energy band from 1.2 to 7.8×10^{-11} photons cm^{-2} s^{-1}, equivalent to 90–560 mcrab (Aharonian et al. 2005a). At the end of 2006 July, the source displayed an anomalously high activity. Preliminary analysis of the HESS data showed an average flux level of 8 crab in the $E > 200$ GeV energy band with flares up to 17 crab during the night of July 27/28, and an average flux level of 1 crab during the night of July 28/29 with smaller activity, while a second outburst occurred in the night of July 29/30 with an average of 5 crab and flares up to 13 crab (Raue et al. 2006; F. A. Aharonian et al. 2007, in preparation). The event was detected also by MAGIC[11] (A. De Angelis 2006, private communication). Following a rapid alert (Benbow et al. 2006), some high-energy satellites pointed at PKS 2155−304.

The *Swift* satellite (Gehrels et al. 2004) performed optical/UV and X-ray follow-up, starting on 2006 July 29 and ending on August 29, with repeated short-exposure pointings. Here we present the results of these observations, a comparison with previous ones when PKS 2155−304 was in a low-activity state, and theoretical modeling of the spectral energy distributions (SEDs).

2. DATA ANALYSIS

The data from the three instruments on board *Swift* have been processed and analyzed with HEASoft version 6.1.2 with the latest calibration files (2006 December 6). Data from individual pointings from the coded-mask hard X-ray detector Burst Alert Telescope (BAT; optimized for the 15–150 keV energy band; Barthelmy et al. 2005) were binned, cleaned from hot pixels and background, and deconvolved. The intensity images were then integrated by using the variance as a weighting factor. PKS 2155−304 was not detected either in individual pointings or in the integrated mosaic image. The upper limit for a 3 σ detection in the 20–40 keV energy band—already corrected for systematics—is 3.3×10^{-10} ergs cm^{-2} s^{-1} (42 mcrab) for the pointing of 2006 July 29 (exposure 6 ks) and 1.6×10^{-10} ergs cm^{-2} s^{-1} (20 mcrab) for the overall mosaic (exposure 30 ks).

Data from the X-Ray Telescope (XRT; 0.3–10 keV; Burrows et al. 2005) were analyzed using the `xrtpipeline` task. XRT automatically switches the operating mode according to the target source flux, changing from window timing (WT; high flux) to photon counting (PC; low flux) with a threshold around 1 mcrab (5×10^{-11} ergs cm^{-2} s^{-1}). The X-ray flux of PKS 2155−304 remained almost always above $\approx 10^{-10}$ ergs cm^{-2} s^{-1} (Fig. 1), and therefore we analyzed only the WT mode data. There are also a few hundreds of seconds exposure in PC mode, but the point-spread function is severely affected by pileup. Nevertheless, we used the source position measured in the images accumulated with PC data as best input for the pipeline of WT mode (without imaging). We selected only the grade 0 (single pixel) events and extracted the spectra only from pointings with exposures greater than 100 s, in order to have the best available statistics. The remaining pointings (i.e., with less than 100 s) are anyway included in the light curve displayed in the top panel of Figure 1, in order to give a better coverage of the time evolution of the source.

Since most of the pointings lasted a few hundreds of seconds, their exposure is insufficient to have data at energies above 4–

[1] INAF/Istituto di Astrofisica Spaziale e Fisica Cosmica, Bologna, Italy; foschini@iasfbo.inaf.it.
[2] INAF/Osservatorio Astronomico di Brera, Milan, Italy.
[3] Dipartimento di Scienze, Università dell'Insubria, Como, Italy.
[4] Department of Physics and Astronomy, School of Computational Sciences, George Mason University, Fairfax, VA.
[5] INAF/Osservatorio Astronomico di Torino, Pino Torinese, Italy.
[6] INAF/Osservatorio Astronomico di Trieste, Trieste, Italy.
[7] Osservatorio Astronomico, Università di Perugia, Perugia, Italy.
[8] NASA Goddard Space Flight Center, Greenbelt, MD.
[9] ASI Science Data Centre, Frascati, Italy.
[10] See http://www.mpi-hd.mpg.de/hfm/HESS.
[11] See http://wwwmagic.mppmu.mpg.de.

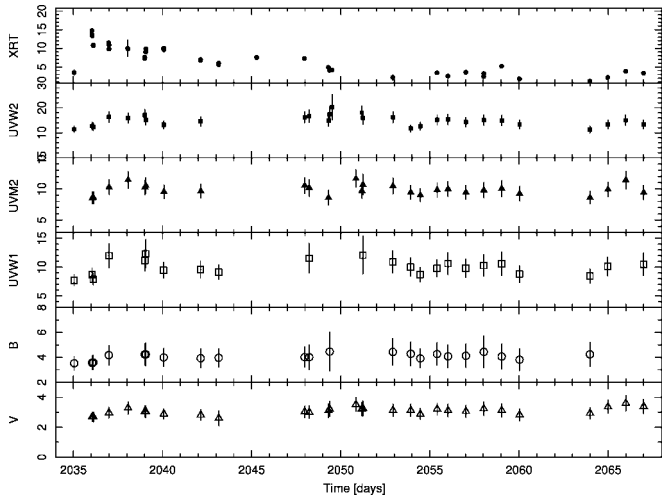

FIG. 1.—Light curves built from data of *Swift* instruments. *From top to bottom*: XRT (0.3–10 keV), UVOT UVW2 (1880 Å), UVM2 (2170 Å), UVW1 (2510 Å), *B* (4390 Å), and *V* (5440 Å). For XRT, only WT mode data have been included, binned to 500 s; a flux of 10^{-10} ergs cm^{-2} s^{-1} is approximately equal to 3.5–4.5 counts s^{-1}. For UVOT, *U* filter data are not included, since for most of the observing time the detector was saturated; for all the other filters, the flux is given in units of 10^{-14} ergs cm^{-2} s^{-1} Å^{-1} and is not corrected for absorption. The mark on abscissa indicates the 00:00:00 UTC of the day; i.e., day 2035 corresponds to 2006 July 29 at 00:00:00.

6 keV, except for the pointing of July 29, where a 5 ks exposure allowed us to have useful signal up to 8 keV. In addition, the XRT response is limited at low energies, because there are still some residual instrumental features around 0.5 keV (Campana et al. 2006). Therefore, the extracted spectra were fitted in the range 0.3–0.45 keV and from 0.6 to 4–8 keV, depending on the statistics, and then the flux was measured in the full 0.3–10 keV band. The results are summarized in Table 1.

For XRT, we note that the observation indicated in Table 1 as "Jul 29/31" actually started on 2006 July 29 at 00:55:42 UTC and ended on 2006 July 31 at 00:01:00 UTC, resulting in an elapsed time of $\approx 1.7 \times 10^5$ s. However, the effective exposure time is only 4916 s. Thus, the spectral data reported in Table 1 refer to the average of the snapshot observations during this period. In addition, we also extracted from this observation the subset of data referring only to the night between July 29 and 30, in order study the data available that are simultaneous to TeV observations. The spectral information about that night are indicated in Table 1 as "Jul 30."

Data from the Ultraviolet/Optical Telescope (UVOT; Roming et al. 2005) were analyzed by using the `uvotmaghist` task with a source region of 6″ for optical and 12″ for UV filters. The background was extracted from an annular region centered on the source and with an inner region equal to the source region plus 2″ and the outer radius equal to 60″. To take into account systematic effects, we added a 10% error in flux (resulting in about 0.1 mag). The results, simultaneous to the X-ray fits, are summarized in Table 1, while complete light curves are shown in Figure 1.

In order to compare X-ray/UV/optical data close to the outburst with data when PKS 2155−304 was not active (i.e., with low X-ray/UV/optical fluxes), we retrieved and analyzed *Swift* observations of the blazar performed in 2006 April. The results of the analysis are reported in Table 1, where the flux difference between April and August observations shows up clearly.

3. DISCUSSION AND INTERPRETATION

3.1. *Overview of Data*

The *Swift* observations of PKS 2155−304 starting on July 29 at 00:55 during the phase of strong TeV activity reported by HESS (Raue et al. 2006; F. A. Aharonian et al. 2007, in preparation) show an initial increase of the X-ray flux, by a factor of 4, between the observation of July 29 and that of July 30 followed by an overall decrease, while optical/UV fluxes show a moderate activity (Fig. 2). No detection in hard X-rays was obtained with BAT.

With respect to the 2006 April observations, XRT recorded a change by a factor of 5, while the UV flux increased by a factor of ≈1.5. For comparison, the HESS observations of 2006 July showed "night-averaged" intensities in the TeV band of factors ≈16 and ≈10 larger than those in 2002–2003 (0.5 crab;

TABLE 1
SUMMARY FOR SWIFT OBSERVATIONS

Date	XRT Exposure (s)	Parameters[a]	F[b]	$\tilde{\chi}^2$/dof	V[c]	B[c]	U[c]	UVW1[c]	UVM2[c]	UVW2[c]
2006 April										
Apr 16	400	2.40 ± 0.09	0.94	1.36/41	13.0	13.4	12.5	12.3	12.6	12.6
Apr 26	155	2.4 ± 0.1	1.31	0.99/20	12.8	13.2	12.3	12.0	12.4	12.3
2006 July–August										
Jul 29/31	4916	2.30 ± 0.03, $1.19^{+0.09}_{-0.11}$, 2.80 ± 0.04	3.43	1.22/319	12.6	13.0	12.1	11.7	12.0	11.9
Jul 30	3276	2.25 ± 0.03, 1.2 ± 0.1, 2.81 ± 0.05	3.61	1.17/287						
Aug 1	351	2.62 ± 0.05	2.90	1.17/93	12.5	<12.8	<12.0	<11.3	11.7	11.7
Aug 2	1842	$2.44^{+0.05}_{-0.07}$, 1.2 ± 0.2, $2.90^{+0.10}_{-0.08}$	2.46	1.06/195	12.5	12.9	<12.0	11.4	11.8	11.7
Aug 3	1605	$2.24^{+0.05}_{-0.13}$, $1.1^{+0.1}_{-0.2}$, $2.75^{+0.06}_{-0.08}$	2.96	1.31/205	12.6	12.9	<12.0	11.6	11.9	11.9
Aug 5	517	2.67 ± 0.05	2.01	0.96/93	12.6	13.0	<12.0	11.6	11.9	11.8
Aug 6	295	2.64 ± 0.08	1.68	0.91/52	12.7	13.0	…	11.6	…	…
Aug 8	439	2.62 ± 0.05	2.29	0.93/91	…	…	…	…	…	…
Aug 10	318	2.58 ± 0.06	2.17	0.91/70	12.6	12.9	<12.0	<11.3	11.8	11.7
Aug 12	139	2.8 ± 0.2	1.27	1.10/17	12.5	12.8	<12.0	<11.3	12.2	11.6
Aug 20	184	2.4 ± 0.1	1.14	1.09/25	12.5	12.9	<12.0	11.6	11.9	11.8
Aug 22	161	2.6 ± 0.1	1.62	1.42/25	12.5	12.9	<12.0	11.5	11.9	11.8

NOTE.—See Fig. 1 for the complete set of data.

[a] Γ for the power-law model or Γ_1, $E_{\rm break}$ (keV), Γ_2, respectively, for the broken power law model. The absorption column is fixed to the Galactic value ($N_{\rm H} = 1.36 \times 10^{20}$ cm^{-2}; Lockman & Savage 1995).

[b] Observed flux in the 0.3–10 keV band (10^{-10} ergs cm^{-2} s^{-1}).

[c] Observed magnitudes. Error 0.1 mag for all, including systematics. Lower limits indicate a saturation of the detector.

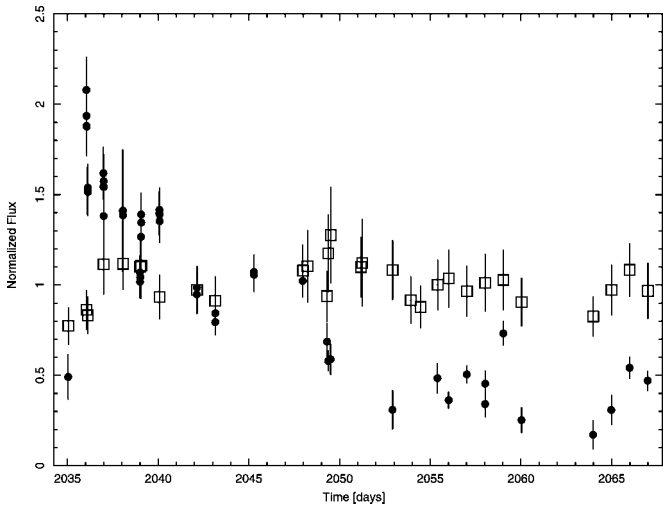

FIG. 2.—Normalized light curves. Filled circles indicate XRT data (0.3–10 keV) normalized to their average in 2006 July–August (7.1 ± 0.6 counts s^{-1}). Open squares indicate the average from UV filters, which are UVW2 (1880 Å), UVM2 (2170 Å), and UVW1 (2510 Å), normalized to $(11.6 \pm 0.6) \times 10^{-14}$ ergs cm^{-2} s^{-1} $Å^{-1}$.

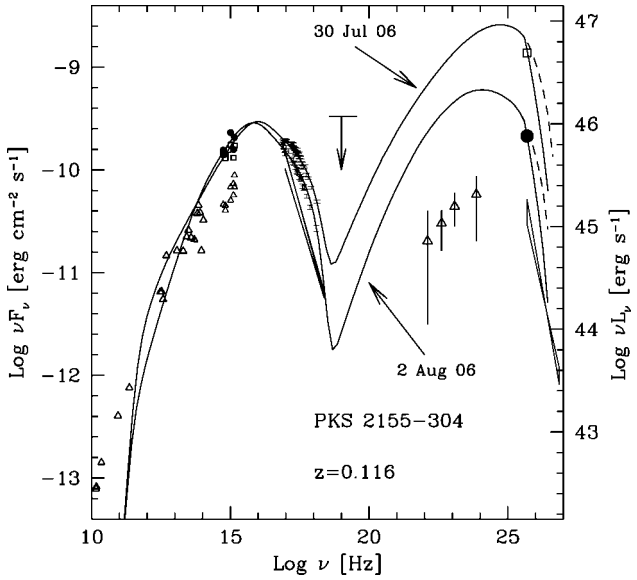

FIG. 3.—SED of PKS 2155−304. The open squares are the quasi-simultaneous data of July 29; the filled circles refer to the observations of August 2. HESS data are from Raue et al. 2006; *Swift* quasi-simultaneous data are from the present work. For comparison, we also report data from the historical records: triangles refer to archival data (references in Chiappetti et al. 1999) and to the HESS TeV spectrum taken in 2003 October–November (Aharonian et al. 2005b), while the other symbols report the *XMM-Newton* data from Foschini et al. (2006). The upper solid line represents the SSC model (see Ghisellini et al. 2002) used to fit the data of 2006 July 29, while the lower solid line represents the model fitted to the data of August 2. Both models include the absorption at TeV energies due to the extragalactic infrared background calculated according to Stecker & Scully (2006). The dashed lines indicate the intrinsic (i.e., not absorbed) spectra. [*See the electronic edition of the Journal for a color version of this figure.*]

Aharonian et al. 2005a, 2005b) but with short flares of up to a factor of 34.

The sparseness of the available data does not allow us to make stringent correlations with TeV data. We note, however, that the initial flare in X-rays taking place between the nights of July 29 and 30 approximately coincides with the second TeV outburst, while a lower amplitude flare in the UV occurs about 1 day later (Fig. 2). Since the UVOT detector was often saturated because of coincidence losses, we cannot exclude the occurrence of other flares with greater amplitude.

3.2. *Spectral Energy Distribution*

With the current data set, we cannot probe the short (5 minute) timescale variability preliminarily reported by HESS (Raue et al. 2006; F. A. Aharonian et al. 2007, in preparation) but can investigate only quantities averaged over timescales of days. We therefore assembled the SED (Fig. 3) using the *Swift* observation tagged as "July 30" that is quasi-simultaneous to the second TeV flare that occurred during the night 2006 July 29/30. We also considered TeV and *Swift* observations performed on August 2, when the blazar activity was declining.

In order to discuss the observed SEDs in terms of changes of relevant physical quantities, we used the model by Ghisellini et al. (2002) to reproduce the SEDs in Figure 3. As generally assumed for this and the other TeV BL Lac objects (e.g., Aharonian 2004), the X-ray emission is attributed to synchrotron radiation and the γ-ray component to the synchrotron self-Compton (SSC) process. The source is assumed to be a sphere of radius R traveling with bulk Lorentz factor Γ at an angle θ with respect to the line of sight, yielding a Doppler factor δ. The magnetic field B is tangled and homogeneous. The distribution of emitting relativistic electrons is computed as the result of a broken power law injection distribution proportional to γ^{-s} between γ_1 and γ_2, and proportional to γ^{-1} below γ_1, subject to radiative cooling occurring in a light crossing time R/c. This injection of relativistic particles corresponds to an injected power $L'_{\rm inj}$ as measured in the comoving frame. The resulting particle distribution $N(\gamma)$ is formed by power-law segments, the steepest of which is proportional to $\gamma^{-(s+1)}$.

All the parameters corresponding to the two models shown in Figure 3 are listed in Table 2. Tavecchio et al. (1998) have shown that, in principle, if the peak frequencies and fluxes of the synchrotron and self-Compton components and the variability timescales are known, then the main parameters for the SSC model are determined. At present, we have only a very partial knowledge of the SED at high energies, resulting in ambiguities in the parameter choice. To fix them, we minimized the luminosity in the self-Compton component assuming an intrinsically steep TeV spectrum. We have also assumed that the variability timescale is ~1 hr, as typically observed in the X-ray band (e.g., Zhang et al. 2002). The much shorter 5 minute variability timescale recently observed in the TeV band should then imply a different additional region/emission process.

The model results show that, while there is some evidence

TABLE 2
SSC MODEL PARAMETERS

Parameter	July 29	August 2
R (10^{15} cm)	5	5
$L'_{\rm inj}$ (10^{42} ergs s^{-1})	1.1	0.3
$\gamma_{\rm break}$ (10^4)	1.5	0.9
$\gamma_{\rm max}$ (10^5)	1.75	1.1
s	2.5	2.6
B (G)	0.27	0.55
$\Gamma_{\rm bulk}$	30	30
θ (deg)	1.7	1.7
δ	33.5	33.5

NOTE.—Parameters for the SSC model by Ghisellini et al. (2002) used to interpolate the SED (Fig. 3); $\Gamma_{\rm bulk}$ is the bulk Lorentz factor, θ is the viewing angle, δ is the Doppler factor, and B is the magnetic field. See the text for more details.

of a flatter X-ray spectrum at higher intensity, the frequency of the synchrotron peak remains at $\approx 10^{15}$–10^{16} Hz, consistent with other observations with much weaker TeV activity (cf. Urry et al. 1997; Chiappetti et al. 1999; Foschini et al. 2006). The low peak frequency value is also a result of the choice of reproducing the optical-UV fluxes. The large difference in TeV fluxes associated with small differences in X-ray spectra requires, in SSC models, an increase of the relativistic electrons accompanied by a decrease of the magnetic field.

The above point is confirmed by a comparison of the present data and model with the *BeppoSAX* observation in 1997 November (Chiappetti et al. 1999), which was performed quasi-simultaneously to the TeV observations by Chadwick et al. (1999), when PKS 2155−304 was at about 0.3 crab (average flux, $E > 300$ GeV). With respect to the parameters derived for the 1997 November episode, the present SSC models yield (see Table 2) a larger Doppler factor ($\delta = 33$ vs. 18), a smaller magnetic field ($B = 0.27$–0.55 vs. 1 G), a flatter index of the electron distribution ($p = s + 1 = 3.5$–3.6 vs. 4.85), and a smaller frequency of the synchrotron peak ($\approx 10^{16}$ vs. 10^{17} Hz) with very similar emitting regions ($R = 5 \times 10^{15}$ vs. 3×10^{15} cm).

In summary, within a simple SSC scheme, the physical parameters of the source changed, in the sense of a harder particle spectrum, a smaller magnetic field, and a greater beaming factor in the 2006 observations. This is required by the different self-Compton to synchrotron luminosity ratio, which was substantially larger in the 2006 observations.

3.3. *Comparison with Other Cases: Mrk 501 in 1997, Mrk 421 in 1998–2000*

It is interesting to compare the present episode with other exceptional activity states that occurred in the past in blazar sources with similar SEDs (Padovani & Giommi 1995). The most striking example to date is the strong TeV activity exhibited by Mrk 501 in 1997 April, observed by the Fred Lawrence Whipple Observatory: during the nights 1997 April 7–19, its flux ($E > 350$ GeV) changed from 0.5 crab to the peak of 3.8 crab that occurred on April 16, with an average of 1.6 crab and no hourly timescale variability (Catanese et al. 1997). *BeppoSAX* observed the simultaneous highly chromatic evolution of the source in X-rays: the flux increased by factors of 4.2, 2.4, and 1.5 in the 13–200, 2–10, and 0.1–2 keV energy bands, respectively, resulting in a frequency shift of the synchrotron peak by 2 orders of magnitude (Pian et al. 1998; Tavecchio et al. 2001). *Rossi X-Ray Timing Explorer* observations revealed also timescale variability down to a few tens of minutes (Xue & Cui 2005). Observations with the *U* filter showed a modest increase of 1% in flux (Catanese et al. 1997). A less extreme, although analogous, behavior was observed in Mrk 421 in 1998–2000. The X-ray and TeV activity were correlated also on a short timescale (Maraschi et al. 1999; Takahashi et al. 2000), with larger amplitude variations in the TeV band. The synchrotron peak appeared to shift to higher energies but not as dramatically as for Mrk 501.

The behavior of PKS 2155−304 appears less striking in X-rays than for the previous two sources but more extreme in the TeV variability. The important questions to be answered concern the understanding of these different "modes" of variability in terms of physical models of the sources. The upcoming γ-ray missions (AGILE and the *Gamma-Ray Large Area Space Telescope*) and the continuous developments of Cerenkov telescope facilities will allow us to define the spectral variability at high energies with unprecedented accuracy. It is, however, mandatory to complement the high-energy data with extensive observations in the X-ray band in order to approach the physical origin of the variability.

4. CONCLUSIONS

We present the observations of the blazar PKS 2155−304 performed by the *Swift* satellite immediately after the giant TeV flare observed by HESS at the end of 2006 July (Raue et al. 2006; F. A. Aharonian et al. 2007, in preparation). The most important result appears to be that, in correspondence with the dramatic TeV activity, the X-ray intensity changed by a factor of 5 but without large spectral changes. In particular, the frequency of the synchrotron peak remained at values similar to those observed in the past (e.g., 1997; Chiappetti et al. 1999), during low TeV activity. Modeling of the SED based on the SSC process in a homogeneous region suggests an increase of the Doppler factor (33 in 2006; 18 in 1997) and of the relativistic electrons associated with a decrease of the magnetic field (0.27 G in 2006; 1 G in 1997).

L. F. thanks V. Bianchin for useful discussions. This research has made use of data obtained from the High Energy Astrophysics Science Archive Research Center (HEASARC), provided by NASA's Goddard Space Flight Center.

REFERENCES

Aharonian, F. A. 2004, Very High Energy Cosmic Gamma Radiation: A Crucial Window on the Extreme Universe (River Edge: World Scientific)
Aharonian, F. A., et al. 2005a, A&A, 430, 865
———. 2005b, A&A, 442, 895
Barthelmy, S. D., et al. 2005, Space Sci. Rev., 120, 143
Benbow, W., Costamante, L., & Giebels, B. 2006, Astron. Tel., 867, 1
Burrows, D. N., et al. 2005, Space Sci. Rev., 120, 165
Campana, S., Beardmore, A. P., Cusumano, G., & Godet, O. 2006, *Swift* XRT CALDB Release Note 09: Response Matrices and Ancillary Response Files (Washington, DC: NASA), http://heasarc.gsfc.nasa.gov/docs/heasarc/caldb/swift/docs/xrt/SWIFT-XRT-CALDB-09.pdf
Catanese, M., et al. 1997, ApJ, 487, L143
Chadwick, P. M., et al. 1999, ApJ, 513, 161
Chiappetti, L., et al. 1999, ApJ, 521, 552
Foschini, L., et al. 2006, A&A, 453, 829
Gehrels, N., et al. 2004, ApJ, 611, 1005
Ghisellini, G., Celotti, A., & Costamante, L. 2002, A&A, 386, 833
Lockman, F. J., & Savage, B. D. 1995, ApJS, 97, 1
Maraschi, L., et al. 1999, ApJ, 526, L81
Padovani, P., & Giommi, P. 1995, ApJ, 444, 567
Pian, E., et al. 1998, ApJ, 492, L17
Raue, M., et al. 2006, in the *INTEGRAL* Workshop on the keV to TeV Connection (Rome: INAF/IASF), http://gri.rm.iasf.cnr.it/keVtoTeV/Docs/33_Mraue.pdf
Roming, P. W. A., et al. 2005, Space Sci. Rev., 120, 95
Stecker, F. W., de Jager, O. C., & Salamon, M. H. 1996, ApJ, 473, L75
Stecker, F. W., & Scully, S. T. 2006, ApJ, 652, L9
Takahashi, T., et al. 2000, ApJ, 542, L105
Tavecchio, F., Maraschi, L., & Ghisellini, G. 1998, ApJ, 509, 608
Tavecchio, F., et al. 2001, ApJ, 554, 725
Urry, C. M., et al. 1997, ApJ, 486, 799
Vestrand, W. T., Stacy, J. G., & Sreekumar, P. 1995, ApJ, 454, L93
Xue, Y., & Cui, W. 2005, ApJ, 622, 160
Zhang, Y. H., et al. 2002, ApJ, 572, 762